Exact and Asymptotic Performance Analysis of WPC Links with Channel Estimation Errors

Danyang Wang, *Student Member, IEEE* and Chintha Tellambura, *Fellow, IEEE*
Department of Electrical and Computer Engineering, University of Alberta, Edmonton, Alberta, Canada
Email: danyang5@ualberta.ca, ct4@ualberta.ca

***Abstract*—In this paper, we investigate the performance of a wireless-powered energy beamforming system with a multiple-antenna access point (AP) and a single-antenna user (SU). The SU first harvests radio frequency (RF) energy from the AP in the downlink (DL) and transmits the information to the AP in the uplink (UL). We consider imperfect estimates and derive the distribution of the received signal-to-noise ratio (SNR) at the AP. The average throughput performance of delay-limited and delay-tolerant modes are evaluated by the outage probability (OP) and ergodic capacity (EC). Finally, analytical and asymptotic results are validated by Monte Carlo simulations.**

***Index Terms*—Channel estimation errors, average throughput, energy harvesting, wireless powered communication network.**

I. Introduction

A. Background and motivation

Wireless-powered communication networks (WPCNs) [1], [2] have emerged as a means to alleviate excess energy use of wireless networks. They exploit the principles of microwave wireless energy transfer and may improve the energy efficiency of battery-constrained wireless nodes. Thus, energy harvesting (EH) from various energy resources is the idea. These include mechanical, solar and radio-frequency (RF) energy sources. However, the solar energy is time variable and the mechanical motion is hard to predict [3]. In contrast, RF energy is ubiquitous. Experimentally, with an isotropic RF transmitter of $4\,\mathrm{W}$ and $1.78\,\mathrm{W}$ power levels, a receiver can harvests $5.5\,\mu\mathrm{W}$ and $2.3\,\mu\mathrm{W}$ energy at the distance $15\,\mathrm{m}$ and $25\,\mathrm{m}$, respectively from the source [4].

Thus, a WPCN may realize operational cost savings by eliminating replacement or recharging of batteries. A key protocol for WPCNs named "harvest-then-transmit" is developed in [5], where the wireless users harvest energy released from the RF signals broadcast by an access-point (AP) in the downlink (DL), and then use the harvested energy to send information to the AP in the uplink (UL). A prototype WPCN system is shown in Fig. 1.

In [1], the average throughput of energy beamforming has been analyzed for a single-user multi-antenna WPCN for delay-limited and delay-tolerant transmission modes. Energy beamforming is utilized to maximize the energy efficiency of single antenna wirelessly powered user and also to enable long distance transmission. Performances of a WPCN over generalized $\kappa-\mu$ fading channels is derived in [6]. In this study, two single-antenna users harvest energy from the AP first and then cooperatively transmit information to the AP. The weighted sum-rate is evaluated to optimize the energy beamforming vector, time allocation, and power allocation.

Channel state information (CSI) is an absolutely critical component of wireless links. In practical systems, perfect CSI is not available and in fact imperfect CSI is the norm [7], [8]. Typically, training (pilot) symbols are sent periodically for CSI estimation purposes. Imperfect CSI in WPCN was studied in [9], [10]. The system proposed in [9] contains a muti-user multi-antenna WPCN. The energy optimization was formulated with consideration of beamforming design, power allocation, antenna selection and time division based on imperfect CSI. The secrecy performance of WPCNs with imperfect CSI has also been investigated [10].

The aforementioned works focus on secrecy imperfect CSI WPCN or the optimization of a WPCN with imperfect CSI, but not the analysis of performance. In this paper, we concentrate on a WPCN system with energy beamforming and imperfect CSI via evaluating the delay-limited mode and delay-tolerant mode.

B. Problem statement and contributions

To the best of our knowledge, the performance of a WPCN due to imperfect CSI has thus far not been available. This gap in understanding of the system performance is problematic. In fact, imperfect CSI can lead to major performance degradation, including diversity and coding gain losses. To quantitatively understand these issues, in this paper, we investigate the two different throughput performances as well as their high signal-to-noise ratio (SNR) performance of a WPCN with energy beamforming and imperfect CSI. In terms of the throughput performance, AP uses delay-limited and delay-tolerant modes.

The main contributions are summarized as follows:

1) We consider a WPCN with energy beamforming and imperfect CSI. The exact close-form expressions are derived for both delay-limited and delay-tolerant modes.
2) Asymptotic analyses are developed for the average throughput. For the delay-tolerant transmission mode, we also obtain the throughput-optimal energy harvesting time in the high SNR regime.

In a nutshell, this paper generalizes the work of [1] to the imperfect CSI case.

Notation: For random variable (RV) X, $f_X(\cdot)$ and $F_X(\cdot)$ denote the probability density function (PDF) and cumulative distribution function (CDF). A circularly symmetric complex Gaussian RV with mean μ and variance σ^2 is $\mathcal{CN}(\mu,\sigma^2)$.

The gamma function $\Gamma(a)$ is given in [11, Eq. (8.310.1)]; $K_\nu(\cdot)$ is the ν-th order modified Bessel function of the second kind [11, Eq. (8.432)]; $G_{pq}^{mn}\left(z \mid {}^{a_1 \cdots a_p}_{b_1 \cdots b_q}\right)$ denotes the Meijer G-function [11, Eq. (9.301)]; $\psi(\cdot)$ is the Euler psi function [11, Eq. (8.36)].

II. System model

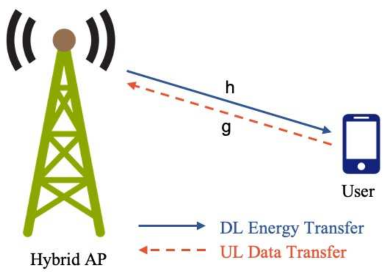

Fig. 1. System Model

In Fig. 1, we consider a single-antenna user (SU) and a multiple-antenna hybrid access point. Both AP and the user are half-duplex nodes. The AP has $N \geq 1$ antennas and uses a maximum ratio combiner (MRC) for UL signal. The fixed battery-less user operates in the harvest-then-transmit protocol [1]. The energy transfer channel, i.e., the AP $\rightarrow$ SU channel, is denoted as $\mathbf{h} = [h_1, \ldots, h_k, \ldots, h_N]^T \in \mathbb{C}^{N\times 1}$, and the information transfer channel, i.e., SU $\rightarrow$ AP channel, is denoted as $\mathbf{g} = [g_1, \ldots . g_k, \ldots, g_N]^T \in \mathbb{C}^{N\times 1}$. The channel coefficients $h_k, g_k \forall k \in [1, N]$ are independent and identically distributed (IID) circularly symmetric complex Gaussian random variables (rvs) with zero-mean and unit-variance, i.e., $h_k, g_k \sim \mathcal{CN}(0, 1)$.

The AP will obtain channel estimates of the true channels $\mathbf{h}$ and $\mathbf{g}$ as $\hat{\mathbf{h}}$ and $\hat{\mathbf{g}}$, respectively, via suitable pilot-assisted channel estimation techniques. Thus, the estimate will have both noise and correlative components. For any true channel $\mathbf{x} \in \{\mathbf{h}, \mathbf{g}\}$, the channel estimate $\hat{\mathbf{x}} \in \{\hat{\mathbf{h}}, \hat{\mathbf{g}}\}$ is related as [12]

$$\hat{\mathbf{x}} = \rho \mathbf{x} + \sqrt{1-\rho^2}\tilde{\mathbf{n}}, \tag{1}$$

where $0 \leq \rho \leq 1$ is the correlation coefficient and $\tilde{\mathbf{n}}$ is an N-dimensional noise vector of IID $\mathcal{CN}(0, 1)$ entries. While $\rho = 1$ denotes perfect channel estimation, $\rho = 0$ is for the worst case estimation, i.e., the estimates are merely noise. The value of ρ is a function of pilot symbols, their power and other factors. For convenience, we assume both uplink estimation and downlink estimation are characterized by the same value of ρ.

For a transmission block of time T, the SU harvests energy for τT duration, and it transmits information for $(1-\tau)T$ duration where $\tau \in [0, 1]$. Without loss of generality, we assume a unit transmission block ($T = 1$). Thus, the total harvested energy at the SU is $E_h = \eta\tau P \frac{||\hat{\mathbf{h}}^H\mathbf{h}||^2}{\hat{\mathbf{h}}^H\hat{\mathbf{h}}}$, where η is the energy conversion efficiency and P is the transmit power of the AP.

By using this harvested energy, the SU transmits the information to the AP in the UL with power P_s which is given as $P_s = \frac{\tau\eta P}{1-\tau}\frac{||\hat{\mathbf{h}}^H\mathbf{h}||^2}{\hat{\mathbf{h}}^H\hat{\mathbf{h}}}$. The received signal at the AP is $y_A = \sqrt{P_s}\mathbf{g}s + \mathbf{n}$, where s is the energy-normalized data symbol and $\mathbf{n}$ is the additive white Gaussian noise (AWGN) term. The AP uses MRC reception to process this signal. The end-to-end SNR can then be derived as

$$\gamma_A = \frac{\tau\eta P}{1-\tau}\frac{1}{\sigma^2}\frac{||\hat{\mathbf{h}}^H\mathbf{h}||^2}{\hat{\mathbf{h}}^H\hat{\mathbf{h}}}\frac{||\hat{\mathbf{g}}^H\mathbf{g}||^2}{\hat{\mathbf{g}}^H\hat{\mathbf{g}}} = \frac{\tau\eta}{1-\tau}\overline{\gamma}XY, \tag{2}$$

where $\overline{\gamma} = \frac{P}{\sigma^2}$, $X = \frac{||\hat{\mathbf{h}}^H\mathbf{h}||^2}{\hat{\mathbf{h}}^H\hat{\mathbf{h}}}$ and $Y = \frac{||\hat{\mathbf{g}}^H\mathbf{g}||^2}{\hat{\mathbf{g}}^H\hat{\mathbf{g}}}$.

III. Statistical distribution results

This section provides necessary statistical distribution results for the use in subsequent derivations throughout the paper.

Lemma 1. *Since $\gamma_A = \frac{\tau\eta}{1-\tau}\overline{\gamma}XY$, the PDF of γ_A is the product of a constant and the rv $Z = XY$. Therefore the PDF can be given by*

$$f_{\gamma_A}(z) = \sum_{n=1}^{N}\sum_{m=1}^{N}\frac{2B_\rho(m,n)\left(\frac{z(1-\tau)}{\tau\eta\overline{\gamma}}\right)^{\alpha(m,n)}}{\frac{\tau\eta}{1-\tau}\overline{\gamma}}K_{n-m}\left(2\sqrt{\frac{z(1-\tau)}{\tau\eta\overline{\gamma}}}\right), \tag{3}$$

where $\alpha(m,n) = \frac{n+m-2}{2}$.

Proof. The PDF of X was derived in [13]

$$f_X(x) = \sum_{n=1}^{N} A(n,\rho,N)x^{n-1}e^{-x}, \quad 0 \leq x < \infty, \tag{4}$$

where $A(n,\rho,N) = \binom{N-1}{n-1}\frac{(1-\rho^2)^{N-n}}{\Gamma(n)}\rho^{2(n-1)}$. As channels are IID, the PDF of Y, $f_Y(y)$, can also be given as (4).

Then the PDF of the product of two rvs X and Y, denoted as $Z = XY$, can be derived as

$$\begin{aligned} f_Z(z) &\stackrel{(a)}{=} \int_0^\infty \frac{1}{\omega} f_X(\omega) f_Y\left(\frac{z}{\omega}\right) d\omega \\ &\stackrel{(b)}{=} \sum_{n=1}^{N}\sum_{m=1}^{N} 2B_\rho(m,n) z^{\frac{n+m-2}{2}} K_{n-m}\left(2\sqrt{z}\right), \end{aligned} \tag{5}$$

where (a) is the formula to find the PDF of the product of two RVs; (b) is obtained by (4), $B_\rho(m,n) \triangleq A(n,\rho,N)A(m,\rho,N)$ and [11, Eq. (3.471.9)].

Since $\gamma_A = \frac{\tau\eta}{(1-\tau)}\overline{\gamma}Z$, the PDF of γ_A can be derived as (3). ■

Corollary 1. *The CDF of γ_A is given by*

$$\begin{aligned} F_{\gamma_A}(x) &\stackrel{(a)}{=} \sum_{n=1}^{N}\sum_{m=1}^{N}\frac{2B_\rho(m,n)}{\frac{\tau\eta}{1-\tau}\overline{\gamma}} \\ &\cdot \int_0^x \left(\frac{(1-\tau)z}{\tau\eta\overline{\gamma}}\right)^{\alpha(m,n)} K_{n-m}\left(2\sqrt{\frac{z}{\frac{\tau\eta}{1-\tau}\overline{\gamma}}}\right)dz \\ &\stackrel{(b)}{=} \sum_{n=1}^{N}\sum_{m=1}^{N}\frac{B_\rho(m,n)}{\left(\frac{\tau\eta}{1-\tau}\overline{\gamma}\right)^{(\alpha(m,n)+1)}}x^{\alpha(m,n)+1} \\ &\cdot G_{1,3}^{2,1}\left(\frac{x}{\frac{\tau\eta}{1-\tau}\overline{\gamma}}\,\middle|\, \begin{matrix} -\alpha(m,n) \\ \frac{n-m}{2}, \frac{m-n}{2}, -\alpha(m,n)-1 \end{matrix}\right), \end{aligned} \tag{6}$$

where (a) follows from the definition of CDF; (b) is obtained by using the equation which expresses $K_v(\cdot)$ in term of $G_{p,q}^{m,n}[\cdot]$ in [1] and [11, Eq. (9.31.5)].

IV. Average Throughput Analysis

In this section, we evaluate the average throughput performance of the system model (Section II). We consider the delay-limited mode and the delay-tolerant mode.

A. Delay-Limited Transmission Mode

1) Exact Throughput Analysis: For delay-limited mode, the AP has a limited cache, and the received signals at the AP should be decoded block by block. Therefore, the outage probability is considered. The outage probability (OP) is given by the probability that the instantaneous throughput, $\log_2(1+\gamma_A)$, falls below a certain predetermined threshold S shown as

$$P_{out} = \Pr\left(\log_2\left(1+\gamma_A\right) < R\right) = F_{\gamma_A}\left(\gamma_{th}\right), \tag{7}$$

where $\gamma_{th} = 2^R - 1$ and $F_{\gamma_A}(y)$ is the CDF of γ_A. The user transmits with a fixed rate R and the effective communication from the user to the AP is

$$\begin{aligned} P_{ave} &= \left(1-P_{out}\right) R\left(1-\tau\right) \\ &= R\left(1-\tau\right)\left[1-\sum_{n=1}^{N}\sum_{m=1}^{N}\frac{B_\rho\left(m,n\right)}{\left(\frac{\tau\eta}{1-\tau}\overline{\gamma}\right)^{\left(\alpha(m,n)+1\right)}}{\gamma_{th}}^{\alpha(m,n)+1}\right. \\ &\left.\cdot G_{1,3}^{2,1}\left(\frac{\gamma_{th}}{\frac{\tau\eta}{1-\tau}\overline{\gamma}}\middle|\begin{array}{c}-\alpha(m,n)\\ \frac{n-m}{2},\frac{m-n}{2},-\alpha(m,n)-1\end{array}\right)\right]. \end{aligned} \tag{8}$$

Although (8) is a closed-form expression, Meijer G-function is complicated to observe the specific relationships between the average throughput and the parameters ρ, τ and $\overline{\gamma}$.

2) Asymptotic Throughput Analysis: In order to gain a simpler result, we derive the asymptotic throughput. To develop this analysis, we need to go back to the definition of γ_A. From (7) the average throughput of the delay-limited transmission mode can be exactly expressed as

$$P_{out} = \Pr\left(XY < \frac{\left(1-\tau\right)\gamma_{th}}{\tau\eta\overline{\gamma}}\right). \tag{9}$$

We use a two-step process to find the asymptotic expression. The first step is to average over X while keeping Y constant. Since the PDF of X is a weight sum (4), the conditional outage may be written as

$$P_{out}\mid_y = \sum_{n=1}^{N} A\left(n,\rho,N\right)\Gamma\left(n\right)\left[1-e^{-\frac{\Delta}{y}}\sum_{l=0}^{n-1}\left(\frac{\Delta}{y}\right)^l\frac{1}{l!}\right], \tag{10}$$

where $\Delta = \frac{\gamma_{th}}{\frac{\tau\eta}{1-\tau}\overline{\gamma}}$; The second step is to average the conditional outage over the PDF of Y when $\overline{\gamma}\to\infty$. This can be done as follows

$$\begin{aligned} P_{out} &= \int_0^\infty P_{out}\mid_y f_Y\left(y\right)dy \\ &\overset{(a)}{=} \sum_{n=1}^{N}\sum_{m=1}^{N} B_\rho\left(m,n\right)\Gamma\left(n\right) \\ &\cdot\int_0^\infty \underbrace{\left[1-e^{-\frac{\Delta}{y}}\sum_{l=0}^{n-1}\left(\frac{\Delta}{y}\right)^l\frac{1}{l!}\right]}_{I} y^{m-1}e^{-y}dy \\ &\overset{(b)}{=} 2\sum_{n=1}^{N}\sum_{m=1}^{N} B_\rho\left(m,n\right)\Delta^{\frac{m+n}{2}}K_{n-m}\left(2\sqrt{\Delta}\right), \end{aligned} \tag{11}$$

where (a) is because of submitting the PDF of Y in (10); (b) is due to the result obtained in Appendix. Then the average throughput $P_{ave} = (1-P_{out})R\left(1-\tau\right)$.

Proof. See Appendix. ■

B. Delay-Tolerant Transmission Mode

1) Exact Throughput Analysis: Delay-tolerant transmission mode is considered for the AP, which has sufficient buffering capacity and can tolerate the delay for decoding the stored signals together. We can evaluate the throughput by calculating the ergodic capacity. Therefore, the average throughput is considered as the product of ergodic capacity and the effective time duration $\left(1-\tau\right)$ for information transmission

$$\begin{aligned} C &= \left(1-\tau\right)\int_0^\infty \log_2\left(1+z\right)f_{\gamma_A}\left(z\right)dz \\ &\overset{(a)}{=} \left(1-\tau\right)\sum_{n=1}^{N}\sum_{m=1}^{N}\frac{2B_\rho\left(m,n\right)}{\frac{\tau\eta}{1-\tau}\overline{\gamma}} \\ &\cdot\int_0^\infty\frac{\ln\left(1+z\right)}{\ln 2}\left(\frac{\left(1-\tau\right)z}{\tau\eta\overline{\gamma}}\right)^{\alpha(m,n)}K_{n-m}\left(2\sqrt{\frac{\left(1-\tau\right)z}{\tau\eta\overline{\gamma}}}\right)dz \\ &\overset{(b)}{=} \left(1-\tau\right)\sum_{n=1}^{N}\sum_{m=1}^{N}\frac{B_\rho\left(m,n\right)}{\frac{\tau\eta}{1-\tau}\overline{\gamma}\ln 2} \\ &\cdot G_{2,4}^{4,1}\left(\frac{1-\tau}{\tau\eta\overline{\gamma}}\middle|\begin{array}{c}-1,0\\ -1,-1,\frac{n-m}{2}+\alpha(m,n),\frac{m-n}{2}+\alpha(m,n)\end{array}\right), \end{aligned} \tag{12}$$

where (a) is obtained by substituting (3) in the definition of capacity; (b) is because of expressing the term $\ln\left(1+x\right)$ and $x^a K_v\left(x\right)$ in Meijer G-functions [14] and then use [11, Eq. (7.811.1)].

2) Asymptotic Throughput Analysis: Asymptotic throughput is derived for $\overline{\gamma}\to\infty$ and $N\to\infty$, respectively to gain insights.

Proposition 1. *The asymptotic capacity of the delay tolerant transmission is given by*

$$C = \frac{1-\tau}{\ln 2}\left[\xi + \ln\eta\overline{\gamma} - \ln\frac{1-\tau}{\tau}\right], \tag{13}$$

where, $\xi = \sum_{n=1}^{N} 2A\left(n,\rho,N\right)\Gamma\left(n\right)\psi\left(n\right)$ *and* $\psi(x)$ *is Euler psi function [11, Eq. (8.360)].*

Proof. Let $C = (1-\tau)C^*$ where

$$\begin{aligned} C^* &= \mathbb{E}\left[\log_2\left(1+\gamma_A\right)\right] \\ &\approx \left[\log_2\frac{\tau\eta}{1-\tau}\overline{\gamma} + \mathbb{E}\log_2\left(X\right) + \mathbb{E}\log_2\left(Y\right)\right] \\ &= \frac{1}{\ln 2}\left[\xi + \ln\eta\overline{\gamma} - \ln\frac{1-\tau}{\tau}\right]. \end{aligned} \tag{14}$$

We find $\mathbb{E}\left[\log(Z)\right] = \left.\frac{d\mathbb{E}\left[Z^{t-1}\right]}{dt}\right|_{t=1}$. For PDF of X and Y, we can find that $\mathbb{E}\left[Z^{t-1}\right] = \sum_{i=1}^{N}\frac{A(i,\rho,N)}{\ln 2}\Gamma\left(i+t-1\right)\psi\left(i+t-1\right)$. From (13), when τ is given, the system throughput is proportional to the logarithm function of the parameter $\overline{\gamma}$ at high SNR. It can be observed that increasing the value of energy harvesting time τ will let the value outside the square brackets decrease but increase the value inside the square brackets. This means the energy harvesting time plays two opposites in (13) and we can find an optimal value for τ to maximize the average throughput for delay-tolerant transmission mode. ∎

Proposition 2. *The optimal energy harvesting time τ^* for delay-tolerant mode at high SNR can be expressed as*

$$\tau^* \approx \frac{1}{1 + W\left(\eta\overline{\gamma}e^{\xi-1}\right)}, \tag{15}$$

where $W(x)$ is the Lambert W function [15].

Proof. First take the first-order derivation over τ to the equation (b) in (13) and let it to zero as $\frac{dC}{d\tau} = 0$; We have $\xi + \ln\eta\overline{\gamma} - \frac{1}{\tau} = \ln\frac{1-\tau}{\tau}$; Then it can be written as $\eta\overline{\gamma}e^{\xi}e^{-\frac{1}{\tau}} = \frac{1-\tau}{\tau}$. Second, after some algebraic manipulations we have $\frac{1-\tau}{\tau} = W\left(\eta\overline{\gamma}e^{\xi-1}\right)$. The final result is given by using $W(\cdot)$ as $\tau = \frac{1}{1+W(\eta\overline{\gamma}e^{\xi-1})}$. $W(x)$ is a monotonically increasing function for $x \geq 0$. From (15), it can be seen that τ^* is inversely proportional to the parameters η, $\overline{\gamma}$ and ξ, and ξ is the function of the number of antennas at the AP. ∎

V. Numerical and Simulation Results

In this section, Monte-Carlo simulations are provided to validate analytical results and evaluate the impacts of key parameters on performances. Without loss of generality, we set transmit block time $T = 1$ and the noise variance $N_0 = 1$.

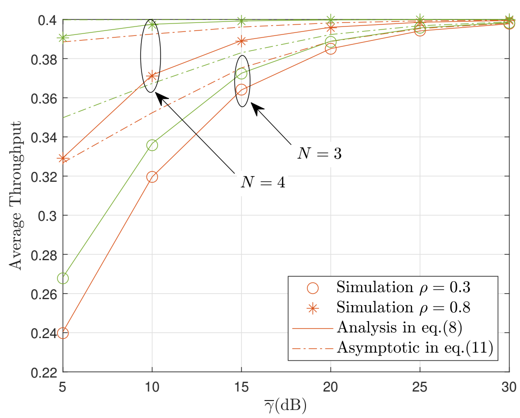

Fig. 2. Average throughput of delay-limited mode versus SNR $\overline{\gamma}$ for $\tau = 0.6$, $\eta = 0.7$ and $R = 1$.

Fig. 2 plots the average throughput of the considered system for delay-limited transmission mode versus the SNR with different numbers of AP antennas and the correlation coefficient. As expected, increasing the transmit power and the number of antenna at the AP can improve the average throughput. It is because more energy can be harvested and higher energy beamforming gain is obtained. In addition, average throughput is also influenced by the correlation coefficient between channel vector and noise. Larger correlation coefficient, better performance. The dotted lines represent the asymptotic analysis of average throughput for $\overline{\gamma} \to \infty$ in (11)

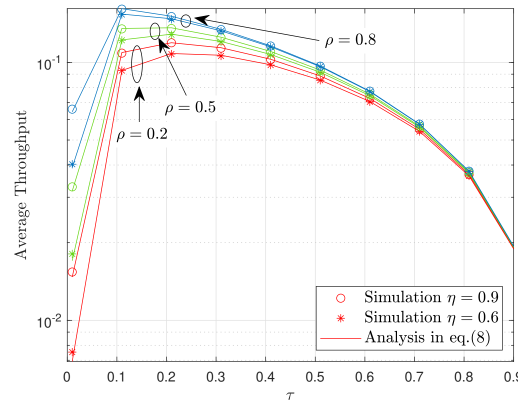

Fig. 3. Average throughput of delay-limited mode versus τ for $N = 3$, $P = 10$ dBm.

and the asymptotic performance is improved while increasing correlation coefficient and transmit power at the AP.

Fig. 3 plots the average throughput of delay-limited mode versus energy harvesting time τ with different correlation coefficients and energy conversion efficiency. We can observe that the average throughput is improved with the correlation coefficient increases because the channel estimation is better. The figure also shows the relation between average throughput and energy conversion efficiency. Obviously, higher energy conversion efficiency helps the user harvest more energy in the DL and it has larger transmitter power to transmit information at the UL. The curves increase first and then decrease with the energy harvesting time increasing.

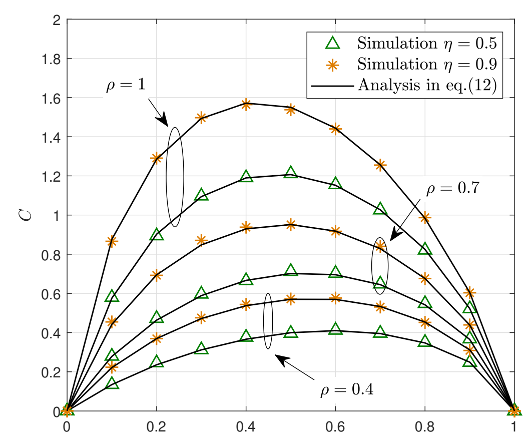

Fig. 4. Average throughput of delay-tolerant mode versus τ for $P = 1$ dBm and $N = 3$.

Fig. 4 plots the average throughput for delay-tolerant mode versus the energy harvesting time τ with different energy conversion efficiencies and correlation coefficients ρ between signal channels and the noise. In the figure, we can see a peek for each curve. It is because in a transmission block of time T, the user harvests energy for τT and transmits information for $(1-\tau)T$, so each case has an optimal energy harvesting time which balances energy harvesting and information processing best. This coincides with our analytical result in (13) and (15). $\rho = 1$ is for perfect channel estimation and $\rho = 0$ is for the worst case estimation, i.e., the estimates are merely noise. Therefore we can observe that the curves with larger ρ have better ergodic capacity. Besides, It is shown than higher energy conversion efficiency also provides better performance of ergodic capacity since the SU can harvest more energy which is used as the transmit power in the UL.

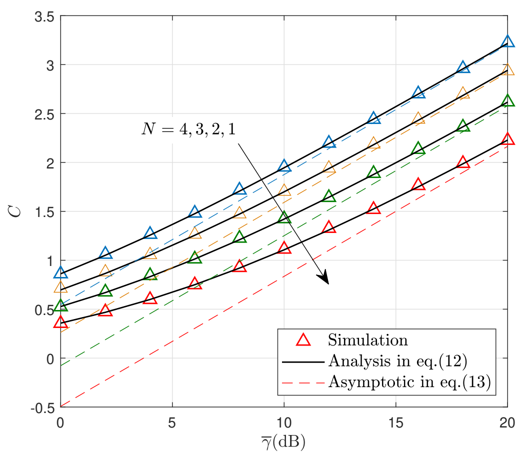

Fig. 5. Average throughput of delay-tolerant mode versus SNR $\overline{\gamma}$ for $\eta = 0.9$, $\tau = 0.6$, $\rho = 0.6$.

Fig. 5 plots the throughput curves for delay-tolerant transmission versus the SNR with different numbers of antenna. As seen in Fig. 5, increasing the transmit power and the number of AP antenna can increase the ergodic capacity of the system. We can also observe that the simulation results match the analysis results we derive in (12). Although the asymptotic curves (13) and the analysis curves (12) have gaps when the transmit power at the AP is small, the asymptotic curves quickly approach the exact one as the transmit power increases.

VI. Conclusion

This paper analyzed the average throughput of a WPCN with channel estimation errors. We analyze the exact and asymptotic performance for delay-tolerant and delay-limit modes. The correctness and effectiveness of these theoretical analysis were verified by simulation results.

Our main findings can be summarized as follows. The average throughput of delay-limited and delay-tolerant modes can be improved by increasing transmit power P, the number of AP antennas, the correlation coefficient and the efficiency of energy harvesting conversion. Under delay-tolerant mode and delay-limited mode, in the numerical results we can find an optimal ratio τ which maximizes the energy harvesting and information transmission.

Appendix

Here, we derive the approximation expression of the term Step (a) in (11). Recall that $\Delta = \frac{\gamma_{th}}{\frac{\tau\eta}{1-\tau}\overline{\gamma}}$, so when $\overline{\gamma} \to \infty$, $\Delta \to 0$ and I can be approximated as

$$I = 1 - e^{-\frac{\Delta}{y}} \sum_{l=0}^{n-1} \left(\frac{\Delta}{y}\right)^l \frac{1}{l!} = e^{-\frac{\Delta}{y}} \left[e^{\frac{\Delta}{y}} - \sum_{l=0}^{n-1} \left(\frac{\Delta}{y}\right)^l \frac{1}{l!} \right] \stackrel{(a)}{=} e^{-\frac{\Delta}{y}} \sum_{l=n}^{\infty} \left(\frac{\Delta}{y}\right)^l \frac{1}{l!} \stackrel{(b)}{\approx} e^{-\frac{\Delta}{y}} \left(\frac{\Delta}{y}\right)^n \frac{1}{n!}, \tag{16}$$

where, (a) is due to Taylor expansion $e^{\frac{\Delta}{y}} = \sum_{l=0}^{\infty} \left(\frac{\Delta}{y}\right)^l \frac{1}{l!}$; When $\Delta \to 0$, the terms for $n \geq n+1$ is smaller than $n = 1$, so we can ignore terms for $n \geq n+1$.

The integral in Step (a) in (11) can be approximated as

$$\begin{aligned} &\int_0^{\infty} \left[1 - e^{-\frac{\Delta}{y}} \sum_{l=0}^{n-1} \left(\frac{\Delta}{y}\right)^l \frac{1}{l!} \right] y^{m-1} e^{-y} dy \\ &\approx \Delta^n \frac{1}{n!} \int_0^{\infty} e^{-\frac{\Delta}{y} - y} y^{m-n-1} dy \\ &= \Delta^{\frac{m+n}{2}} K_{n-m} \left(2\sqrt{\Delta}\right), \end{aligned} \tag{17}$$

which is obtained by using [11, 3.471.9]. By substituting this in (11), we obtain the final result.

References

[1] W. Huang, H. Chen, Y. Li, and B. Vucetic, "On the performance of multi-antenna wireless-powered communications with energy beamforming," *IEEE Trans. Veh. Technol.*, vol. 65, no. 3, pp. 1801–1808, Mar. 2016.

[2] Z. Chu, F. Zhou, Z. Zhu *et al.*, "Energy beamforming design and user cooperation for wireless powered communication networks," *IEEE Commun. Lett.*, vol. 6, no. 6, pp. 750–753, 2017.

[3] S. Bi, Y. Zeng, and R. Zhang, "Wireless powered communication networks: An overview," *IEEE Wireless Commun.*, vol. 23, no. 2, pp. 10–18, 2016.

[4] M. A. Hossain, R. M. Noor, K.-L. A. Yau *et al.*, "A survey on simultaneous wireless information and power transfer with cooperative relay and future challenges," *IEEE Access*, vol. 7, pp. 19 166–19 198, Feb. 2019.

[5] H. Ju and R. Zhang, "Throughput maximization in wireless powered communication networks," *IEEE Trans. Wireless Commun.*, vol. 13, no. 1, pp. 418–428, 2013.

[6] N. Deepan and B. Rebekka, "On the performance of wireless powered communication networks over generalized κ- μ fading channels," *Physical Communication*, vol. 36, p. 100759, 2019.

[7] G. Wang, Q. Liu, R. He, F. Gao, and C. Tellambura, "Acquisition of channel state information in heterogeneous cloud radio access networks: challenges and research directions," *IEEE Wireless Commun.*, vol. 22, no. 3, pp. 100–107, 2015.

[8] G. Wang, F. Gao, Y.-C. Wu, and C. Tellambura, "Joint cfo and channel estimation for ofdm-based two-way relay networks," *IEEE Trans. Wireless Commun.*, vol. 10, no. 2, pp. 456–465, 2010.

[9] Z. Chang, Z. Wang, X. Guo, Z. Han, and T. Ristaniemi, "Energy-efficient resource allocation for wireless powered massive MIMO system with imperfect CSI," *IEEE Trans. Green Commun. Netw.*, vol. 1, no. 2, pp. 121–130, 2017.

[10] Y. Huang, P. Zhang, Q. Wu, and J. Wang, "Secrecy performance of wireless powered communication networks with multiple eavesdroppers and outdated CSI," *IEEE Access*, vol. 6, pp. 33 774–33 788, 2018.

[11] I. S. Gradshteyn and I. M. Ryzhik, *Table of Integrals, Series, and Products, 7th edition*. Academic Press, 2007.

[12] G. Pan, H. Lei, and Y. Deng, "On secrecy performance of MISO SWIPT systems with TAS and imperfect CSI," *IEEE Trans. Commun.*, vol. 64, no. 3, pp. 3831–3843, 2016.

[13] M. J. Gans, "The effect of gaussian error in maximal ratio combiners," *IEEE Trans. Commun. Technol.*, vol. 19, no. 4, pp. 492–500, Aug. 1971.

[14] K. Huang and V. K. N. Lau, "Enabling wireless power transfer in cellular networks: Architecture, modeling and deployment," *IEEE Trans. Wireless Commun.*, vol. 13, no. 2, pp. 902–912, Feb. 2014.

[15] I. Chatzigeorgiou, "Bounds on the Lambert function and their application to the outage analysis of user cooperation," *IEEE Commun. Lett.*, vol. 17, no. 8, pp. 1505–1508, Aug. 2013.